Int. J. Electrochem. Sci., 11 **(2016)** 1121 - 1134

International Journal of
ELECTROCHEMICAL
SCIENCE
www.electrochemsci.org

Electrochemical Oxidation Degradation of Methyl Orange Wastewater by Nb/PbO_2 Electrode

Huimin Yang[1], *Jintao Liang*[2], *Li Zhang*[1], *Zhenhai Liang*[1,*]

[1] College of Chemistry and Chemical Engineering, Taiyuan University of Technology
[2] Shanxi Survey and Design Institute of Water Conservancy and Hydropower
Taiyuan, Shanxi, 030024, China
[*]E-mail: liangzhenh@sina.com, liangzhenhai@tyut.edu.cn

Received: 29 October 2015 / *Accepted:* 22 November 2015 / *Published:* 1 January 2016

Nb/PbO_2 electrode was prepared through electrodeposition method and used as anode in the reaction of electrochemical degradation of methyl orange (MO). The SEM, XRD and cyclic voltammetry tests showed that Nb/PbO_2 electrode surface was dense, uniform and mainly composed of β-PbO_2 with a small amount of α-PbO_2, as well as it has good catalytic effect on degradation of MO. The effects of supporting electrolyte, degradation temperature, current density and pH value on the decolourisation efficiency of MO had also been studied. Results revealed that at initial pH=6.0, 45 ^{o}C temperature, 50 $mA \cdot cm^{-2}$ current density, 0.08 $mol \cdot L^{-1}$ electrolyte (Na_2SO_4) concentration, and 30 min electrolysis time, the colour removal efficiency and COD removal reached 99.6% and 72.6%, respectively. The reaction mechanism of electrocatalytic MO degradation by Nb/PbO_2 electrode mainly involved the OH radical attack of parent molecules, and the degradation followed pseudo-first-order kinetics.

Keywords: Methyl orange; electrochemical degradation; Nb/PbO_2 electrode; kinetics; hydroxyl radicals

1. INTRODUCTION

Textile wastewater usually contains some contaminants, such as acids, bases, dissolved solids, toxic compounds and coloured materials. These contaminants must be removed before the wastewater can be discharged. There are many chemical, biological, and physicochemical methods have been used to treat dye-containing wastewaters[1,2]. They have individual advantages but also have certain constraints that cause inadequate effectiveness when applied individually. Generally, chemical or physicochemical methods will cause secondary pollution or need post-treatment, whereas for the reason of microbial inhibition, the treatment efficiency of biological approaches was very low[3,4].

Advanced oxidation processes have been proposed to be the alternative and efficient methods for the treatment of wastewater that contains toxic or non-biodegradable pollutants. There are many processes have been investigated, such as wet air oxidation, ozonation, electrochemical oxidation, Fenton oxidation and their combined processes[5–7]. By comparison, electrochemical oxidation has received widespread concern for biorefractory pollutant abatement. Electrochemical oxidation is an efficient pathway to treat dye wastewater. Given its certain significant advantages such as easy operation, moderate temperature and pressure requirements, high degradation efficiency, no chemical reagents needed and avoiding secondary pollution[8-12].

Anode materials have important functions on the electrochemical degradation process of organic pollutants. Platinum electrodes[13], diamond and metal alloy electrodes[14], and boron-doped diamond electrodes[15,16] are commonly used as anode materials for wastewater treatment. Activated carbon[17], single-walled carbon nanotubes[18], and titanium-based dimension-stable electrodes[19] are other conventionally used electrode materials. As a type of anode material, Nb/PbO_2 electrode has been used in the electrochemical degradation of 4-chloroguaiacol[20] and chlorpyrifos[21]. However, there is no reports about the application of Nb/PbO_2 electrode as anode material used in the electrochemical degradation reaction of MO.

In the present work, Nb/PbO_2 electrode was prepared via electrodeposition and used to decompose MO dye via electrochemical method. The optimal parameters (such as initial pH, current density, reaction temperature and electrolyte concentration) in the process of electrochemical degradation MO containing wastewater were also studied. The low-cost and easy processing of Nb/PbO_2 electrode increase the attractiveness of this technique in comparison with other processes.

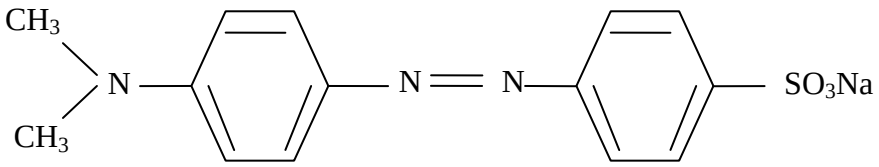

Figure 1. Chemical structure of methyl orange.

2. EXPERIMENT

2.1 Reagents

The chemical reagents used in the experiment are of analytical grade and used without further purification. MO was obtained from Beijing Chemical Reagent Company, and its chemical structure is shown in Fig.1. The MO concentration in the simulated wastewater used in the experiments was 30 $mg \cdot L^{-1}$. Na_2SO_4 solution was used as supporting electrolyte, and NaOH or H_2SO_4 were used to adjust the pH value of electrolyte.

2.2 Preparation of Nb/PbO_2 electrode

2.2.1 Niobium surface treatment

In order to prepare a good adhesive lead dioxide film, niobium substrate need to be pretreated according to the following procedures: First, a Nb sheet (20 mm × 10 mm × 1 mm) was polished by 320-grit paper strips, then the Nb sheet was cleansed with water and acetone. Second, the sheet was ultrasonically rinsed in double-distilled water for 10 min. Finally, the Nb substrate was successively soaked 30 s in hydrofluoric acid (5% weight) and sulfuric acid (20% weight) at room temperature and then abundantly rinsed with double-distilled water.

2.2.2 Electrochemical deposition of PbO_2

Put the pretreated Nb substrate as anode in a single-compartment Pyrex glass cell (100 mL) contain 1M $Pb(NO_3)_2$ aqueous solution, then thermo-regulated electrochemical anodization at 65 °C. The cathode is a graphite electrode. The Nb/PbO_2 electrode was obtained at 10 $mA \cdot cm^{-2}$ in 1.5 h, then at 20 $mA \cdot cm^{-2}$ in 45 min, and finally at 50 $mA \cdot cm^{-2}$ in 15 min. Lead dioxide was successfully deposited on the pretreated Nb substrate. The obtained PbO_2 deposits was mat gray, adherent, regular, and uniform.

2.3 Electrolysis of MO

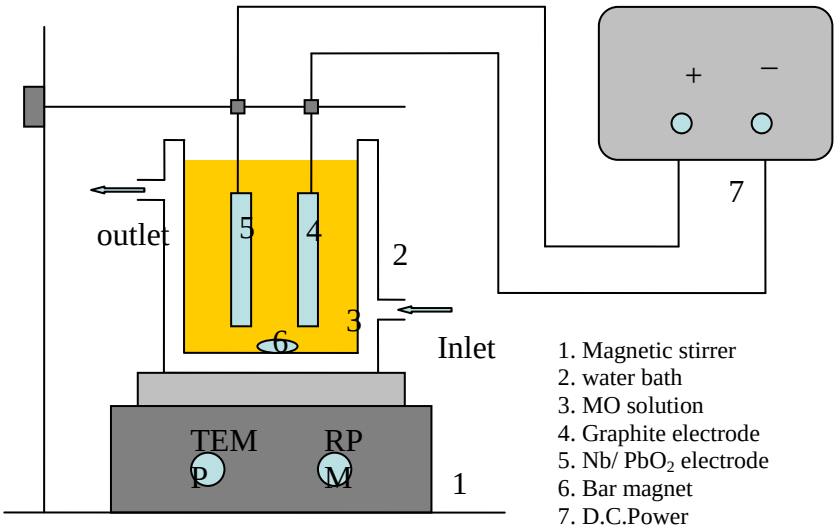

Figure 2. Schematic diagram of experimental set-up.

All solutions were prepared with deionised water. The supporting electrolyte was Na_2SO_4 solution. The MO concentration used in the experiments was 30 $mg \cdot L^{-1}$. Galvanostatic electrolyse process of MO aqueous solution (100 mL) was carried out in the thermostatted cell (Fig. 2). The

graphite electrode (20 mm × 10 mm × 10 mm) was chosen as cathode, and prepared Nb/PbO_2 electrode as anode. The total area of the anode is 4 cm^2. The applied current densities range was 10–50 $mA \cdot cm^{-2}$ using a DC power supply. The pH value of the electrolyte was adjusted through the addition of H_2SO_4 or NaOH solution. The total degradation time was 60min, take a sample every 10 minutes, then determine the MO concentration using an ultraviolet–visible (UV–vis) spectrophotometer at 465 nm wavelength. The chemical oxygen demand(COD) content of MO before and after degradation was detected through dichromate titrimetric standard method, the COD content before degradation was marked COD_0, the COD content after degradation was marked COD_t, the calculated formula was $\eta = \frac{COD_0 - COD_t}{COD_0} \times 100\%$.

2.4 Analytical measurements

The JEOL JSM-7001F scanning electron microscope (SEM, 10 kV) was used to investigate the surface morphology of prepared Nb/PbO_2 electrode. The X-ray diffraction (XRD) data were collected on a D/max-2500 power diffractometer(Cu Kα radiation, 40 kV, 100 mA, $8^o \cdot min^{-1}$). In the experiment, the pH value of solution was tested using a pHS-2C meter (Shanghai, China). The MO concentration was determined through the ultraviolet–visible (UV–vis) spectrophotometer (Cary50, Varian Inc., US). The cyclic voltammetry(CV) curves were measured using a conventional three-electrode cell by the CHI660D electrochemical workstation, prepared Nb/PbO_2 electrode was used as working electrode, platinum electrode as counter electrode, a saturated calomel electrode (SCE) as reference electrode.

3. RESULTS AND DISCUSSION

3.1 Characterization of Nb/PbO_2 electrode

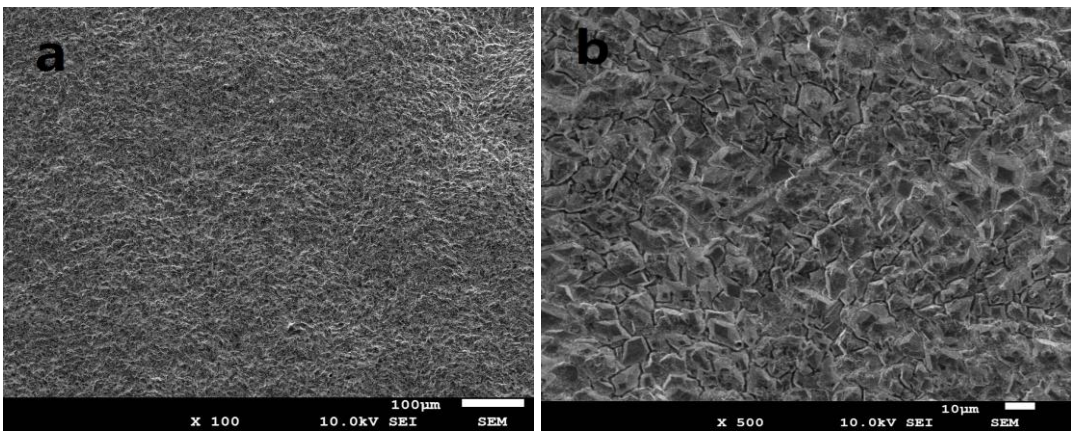

Figure 3. The surface morphology of Nb/ PbO_2 electrode.

Fig. 3 shows the SEM micrographs of Nb/PbO_2 electrode. Based on Fig. 3a, the electrode surface is dense and uniform, which not only ensures the close association between the active layer and

the substrate but also prevents reactive oxygen from penetrating into the surface niobium and guards against the production of non-conductive niobium oxide in the anode, leading to electrode deactivation or coating fall off. From Fig. 3b, the morphology of Nb/PbO_2 electrode displays a mushroom cloud shape. This structure provides a more specific surface and good physical performance for the electrocatalytic degradation of MO.

PbO_2 is a polymorphic material with two crystalline forms: β-PbO_2 and α-PbO_2. Generally, orthorhombic α-PbO_2 and tetragonal β-PbO_2 are found in PbO_2. The XRD patterns of the prepared Nb/PbO_2 electrode was shown in Fig. 4. The surface layer is mainly composed of β-PbO_2 with a small amount of α-PbO_2. The peaks at 2θ = 25.5, 32, 49.7, 52.4, 63, 67.3 are the main diffraction peaks of tetragonal β-PbO_2. Certain weak peaks indicate the presence of orthorhombic α-PbO_2 at 2θ = 36.5, 56. The conductivity of β-PbO_2 is almost ten times higher than that of α-PbO_2, which demonstrates that the increasing content of the β-PbO_2 will result the conductivity of PbO_2 enhanced. Therefore, Nb/PbO_2 electrode exhibits good electrical conductivity.

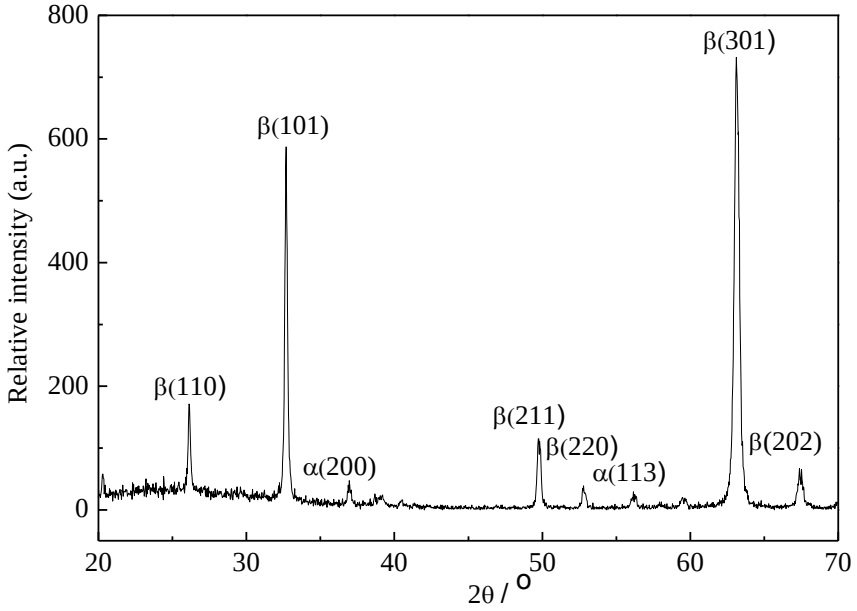

Figure 4. XRD patterns of Nb/ PbO_2 electrode.

3.2 Cylic Voltammetry measurements

The CV curves of Nb/PbO_2 electrode was obtained in 0.08 mol·L^{-1} Na_2SO_4 with and without 5 mg·L^{-1} MO are shown in Fig. 5. The redox peaks at 0.78 V and 0.89 V (vs. SCE) are observed in blank electrolyte, which represent the redox processes of Pb(IV)/Pb(II) couple. However, when MO is present, a new oxidation peak appears at 1.16 V potential. This oxidation peak may be result from the oxidation reaction of MO molecules on the Nb/PbO_2 anode, which clearly indicate that Nb/PbO_2 electrode has good catalytic effect on degradation of MO.

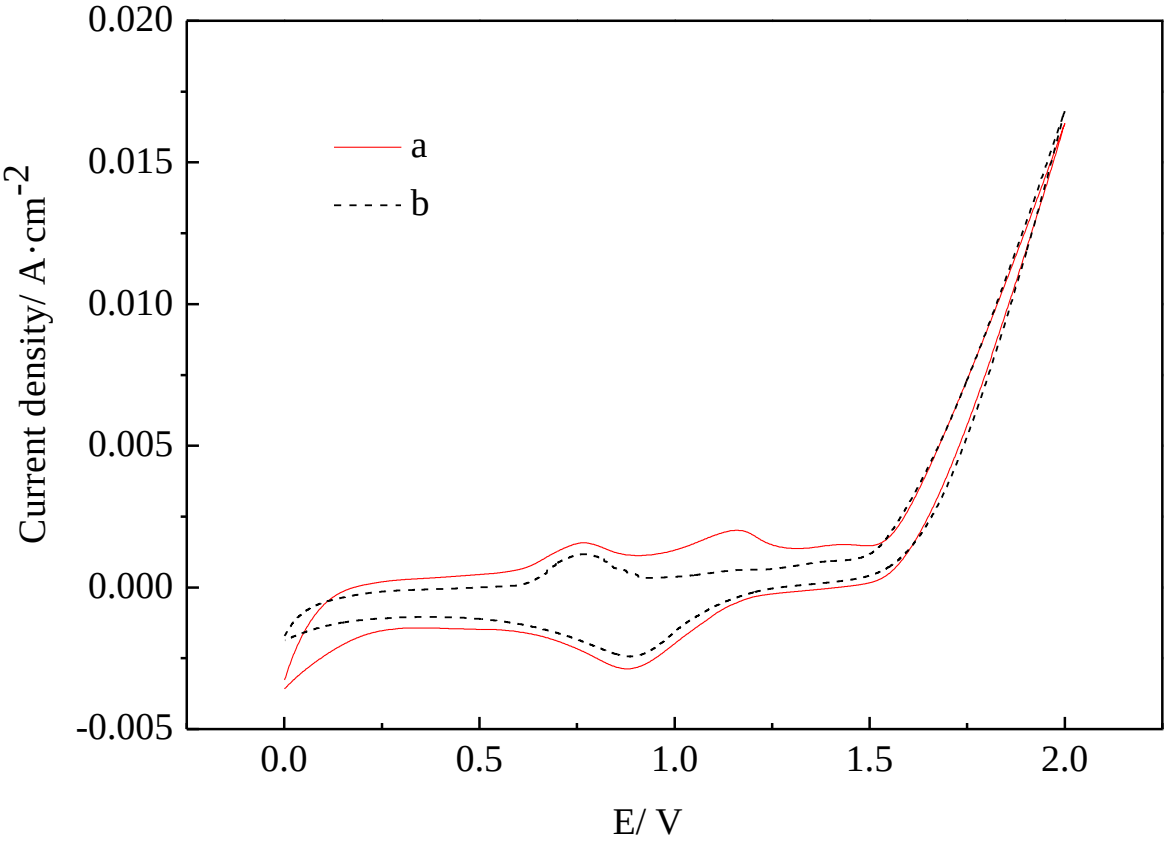

Figure 5. CV curves of Nb/ PbO_2 electrode in 0.08 mol·L^{-1} Na_2SO_4 with 5 mg·L^{-1} MO(a) and without MO(b) at the scan rate of 50 mV·s^{-1}.

3.3 Effect of supporting electrolyte

To confirm the effect of supporting electrolyte (Na_2SO_4) concentration on the electrochemical degradation of MO, experiments were performed at pH=6.0 and a current density of 30 mA·cm^{-2} with different Na_2SO_4 concentrations. As shown in Fig.6, the efficiency of MO removal increases initially with the increase in Na_2SO_4 concentration, this is because the generation of peroxodisulfates. SO_4^{2-} ions are easily oxidized at PbO_2 anode to form persulfate (Eq. (1)) [22, 23]. They are all very powerful oxidants which can greatly oxidize organic matter [24] and cause higher MO removal efficiencies.

$$2SO_4^{2-} \rightarrow S_2O_8^{2-} + 2e^- \quad (1)$$

However, MO removal efficiency decreases to a low value when Na_2SO_4 concentration exceeds 0.08 mol·L^{-1}. When the Na_2SO_4 concentration increases further, too much SO_4^{2-} ions induce more H_2O_2 generation resulting from the generation of $S_2O_8^{2-}$. The electro-generated H_2O_2 could be oxidised to O_2 at the anode, resulting in the decrease of generating radical, such as $HO_2\cdot$ or $OH\cdot$ [25]. Therefore, 0.08 mol·L^{-1} is inferred as the optimal concentration of Na_2SO_4 for maximum MO removal rate.

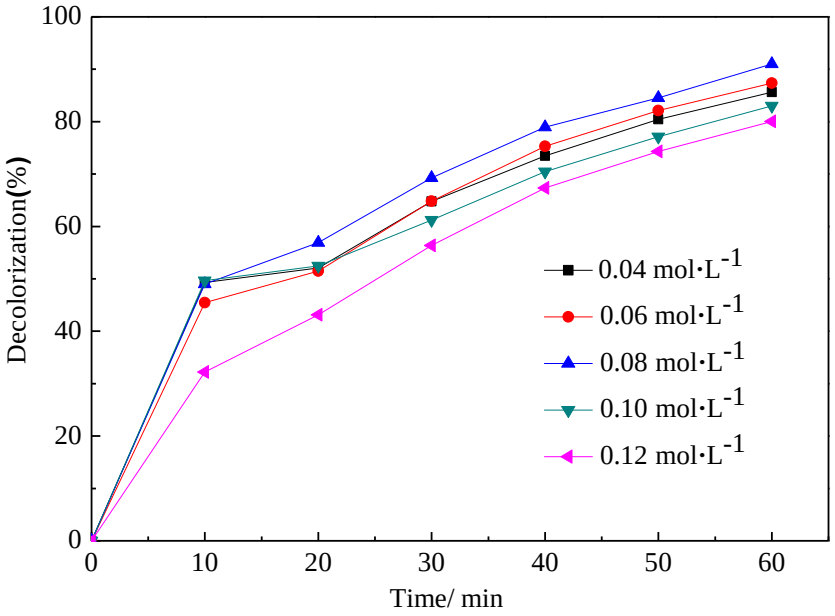

Figure 6. The effect of Na_2SO_4 concentration on MO removal efficiency. (25°C, pH=6, MO concentration: 30 mg·L^{-1}; current density: 30 mA·cm^{-2}).

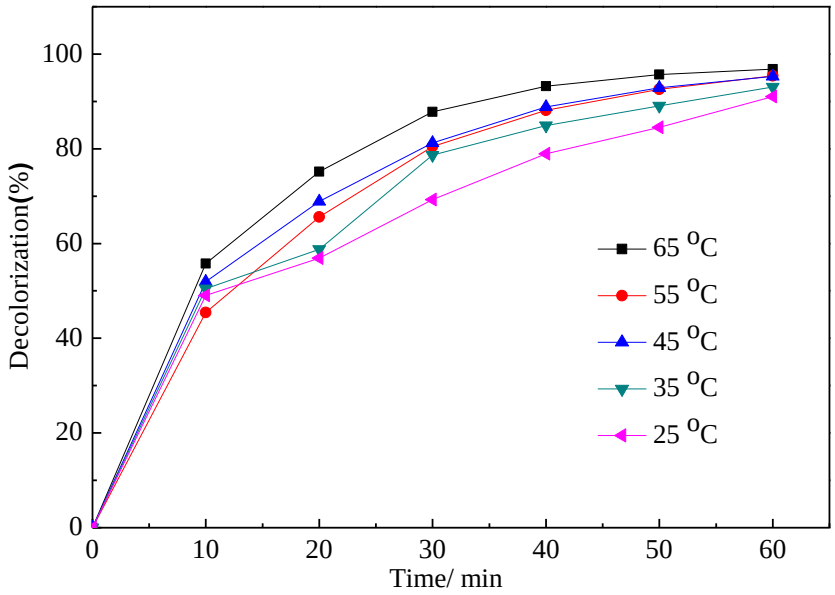

Figure 7. The effect of reaction temperature on MO removal efficiency with time. (pH: 6; MO concentration: 30mg·L^{-1}; current density: 30 mA·cm^{-2}; Na_2SO_4: 0.08 mol L^{-1}).

3.4 Effect of temperature

The decolourisation efficiency at different degradation temperatures are shown in Fig.7. Generally speaking, it can enhance the catalytic activity of the catalyst at high temperature, the MO removal efficiency and evolution of oxygen will increase with temperature rises. However, when the reaction temperature increases to 45 °C, the increase rate of MO degradation efficiency is not too obvious, Thus, improving the MO degradation efficiency by increasing the temperature further not

only wastes energy but also does not lead to good results. Hence, the optimal MO degradation temperature is 45 °C.

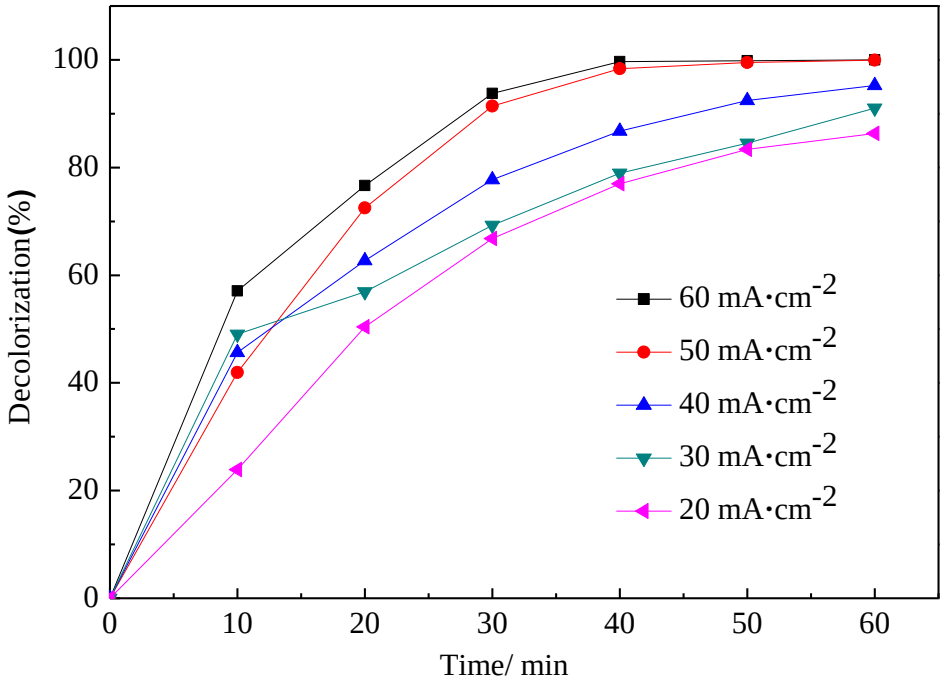

Figure 8. The effect of current density on MO removal efficiency. (25 °C, pH=6, 30 mg· L^{-1} MO, 0.08 mol·L^{-1} Na_2SO_4 solution).

3.5 Effect of current density

Current density play a very important role in the electrochemical oxidation process. 20–60 mA·cm^{-2} current densities were applied to investigate the influence of current density in the electrocatalytic degradation process of MO. It can be clearly seen from Fig. 8, the MO removal efficiency significantly increases with the increase in current density. The MO removal efficiencies after 40 min reach 77.0%, 79.0%, 86.7%, 98.3%, and 99.6% at 20, 30, 40, 50, and 60 mA·cm^{-2}, respectively. This result can be ascribed to that high current density can produce more strong-oxidation free radicals, such as peroxodisulfates or hydroxyl radicals.

A sharp increase in MO removal efficiency is observed when the current density lower than 50 mA·cm^{-2}. When the current density reaches 50 mA·cm^{-2}, MO could be removed completely after 40 min of electrolysis. Only a slight increase in MO removal efficiency is observed when the current density exceeds 50 mA·cm^{-2}, which can be attributed to the fact that the oxidation of H_2O to O_2 (Eq. (2)) is favoured over OH· formation at high current density [26], and an higher current density will enhance the over potential required for the generation of oxidants and consume more energy. Therefore, the optimal current density for electrocatalytic degradation reaction of MO is 50 mA·cm^{-2}.

$$2H_2O \rightarrow O_2 + 4H^+ + 4e^- \quad (2)$$

3.6. Effect of initial pH values

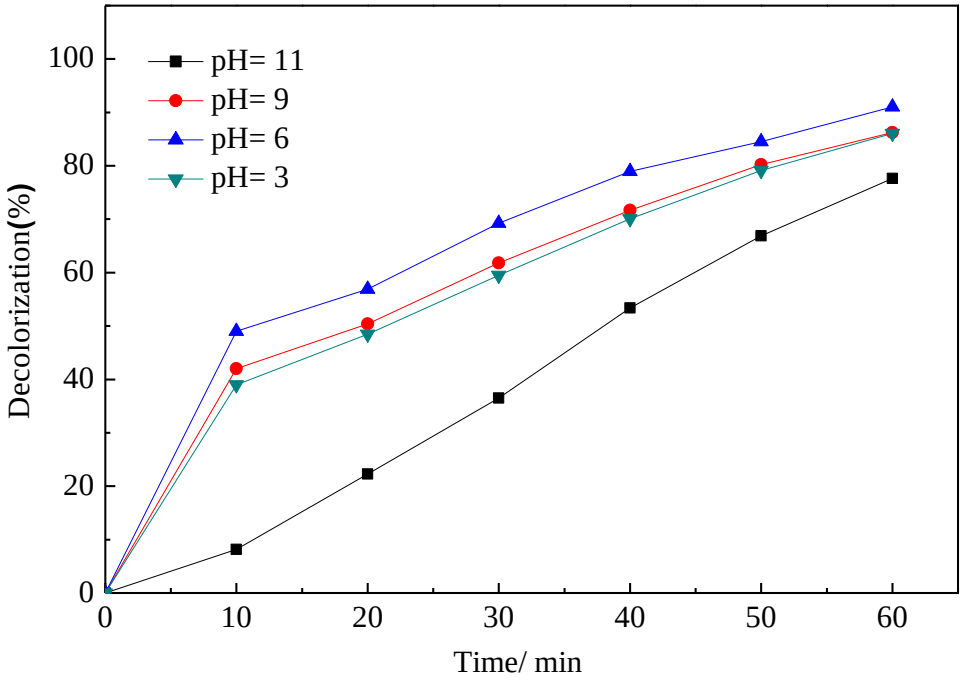

Figure 9. The effect of current density on MO removal efficiency. (25°C, 30 mA·cm^{-2}, 30 mg·L^{-1} MO, 0.08 mol ·L^{-1} Na_2SO_4.).

MO molecular has two chemical structures at different solution pH. When the pH value low, the main form of MO have quinoid structure, and azo structure at high pH[27]. So the initial pH is another important parameter in the electrochemical oxidation process. Therefore, the effect of initial pH values ranging from 3 to 11 on the MO degradation rate was studied. H_2SO_4 and NaOH solutions were used for pH adjustments. Apparently, an appropriate pH benefits the cleavage of the azo bond, and the results are shown in Fig. 9.

A significant difference in decolourisation is noted with the changes in the electrolyte initial pH. The MO molecules readily decompose when the solution pH is 6.0. The decomposition reaction of MO is more easily happened in appropriate acidic solution than in alkaline solution. A competition for oxygen evolution reaction occurs with the oxidative degradation of organic matter on the anode. Oxygen evolution reaction is difficult in acid solutions with high oxygen evolution potential. Conversely, oxygen evolution reaction tends to occur in alkaline environment with low oxygen evolution potential. Hence, increasing the solution pH will decrease the oxygen evolution potential, meanwhile increase the oxygen evolution rate at the surface of anode, which will slow down the diffusion rate of the organics towards the anode[28]. In addition, electrolytes are consumed excessively in an alkaline environment, and the conductivity of the solution is subsequently reduced for the lack of electrolyte[29].

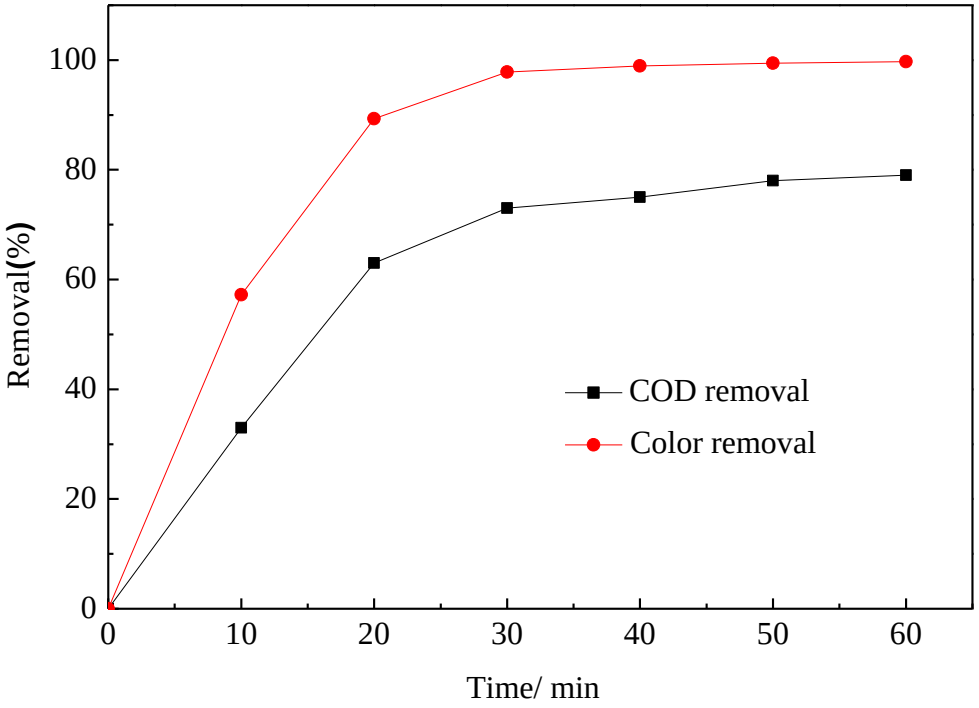

Figure 10. The COD and color removal at optimal conditions.

3.7 Electrolysis time on COD and color removal

The influence of time on the COD and colour removal under the optimal conditions (45 ^{o}C, initial pH=6.0, 0.08 mol·L^{-1}Na_2SO_4, 30 mg·L^{-1}MO, 50 mA·cm^{-2}) was investigated. As shown in Fig. 10, the COD content and colour removal increased with the electrolysis time going. After 30 min, the COD content and colour removal reached the maximum of 72.6% and 99.6%, respectively.

3.8 Analysis of MO degradation kinetics

The oxidation degradation of MO is attributed to the electrochemical generation of the radicals on the anode surface. A large amount of hydroxyl radicals are produced when water electrolysis and readily react with the organic molecules adsorbed on the anode[27, 30]. Therefore, the reaction between $OH^{\bullet}$ radical and MO was the key process in MO electrochemical degradation. The general pathway of MO degradation is as follows: $OH^{\bullet}$ is generated at the Nb/PbO_2 electrode; subsequently, the conjugated structure of azo bond will disconnect when it react with $OH^{\bullet}$; Part of the MO reduction intermediates will further oxidized into a series of aromatic metabolites, which are finally mineralised to CO_2 and H_2O. The reactions[31, 32] are described in Fig. 11 .

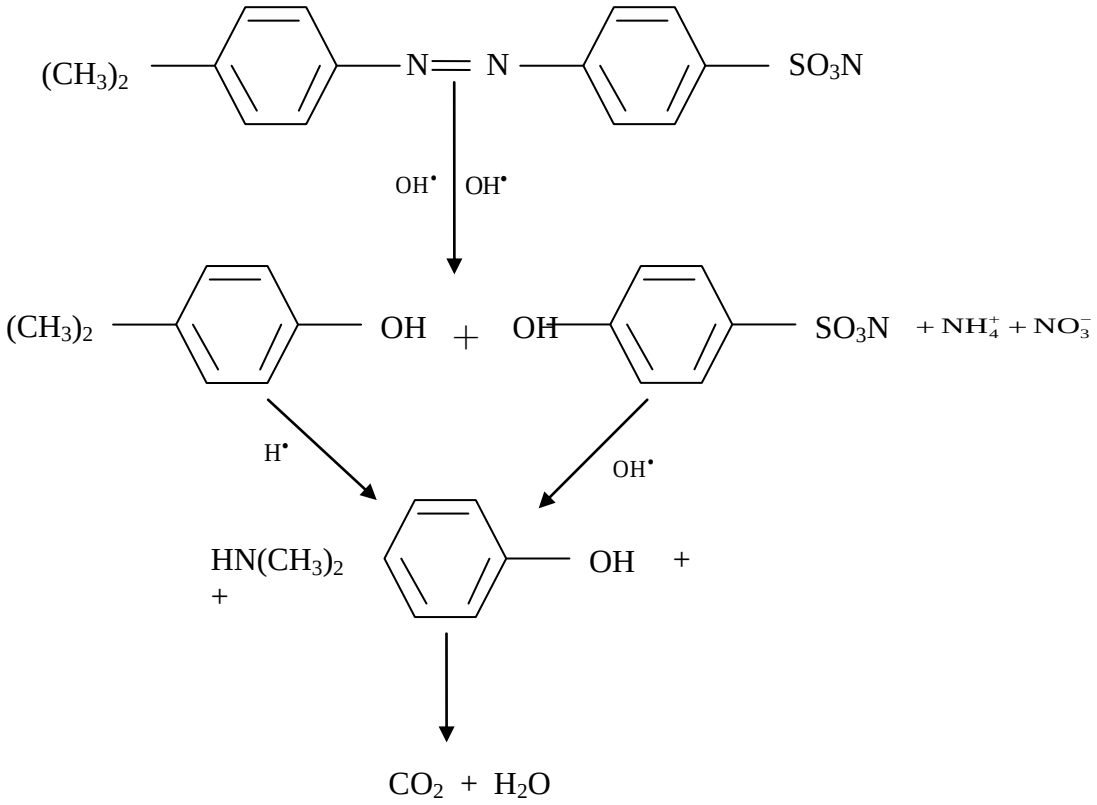

Figure 11. Reaction pathway of electro-catalytic degradation MO.

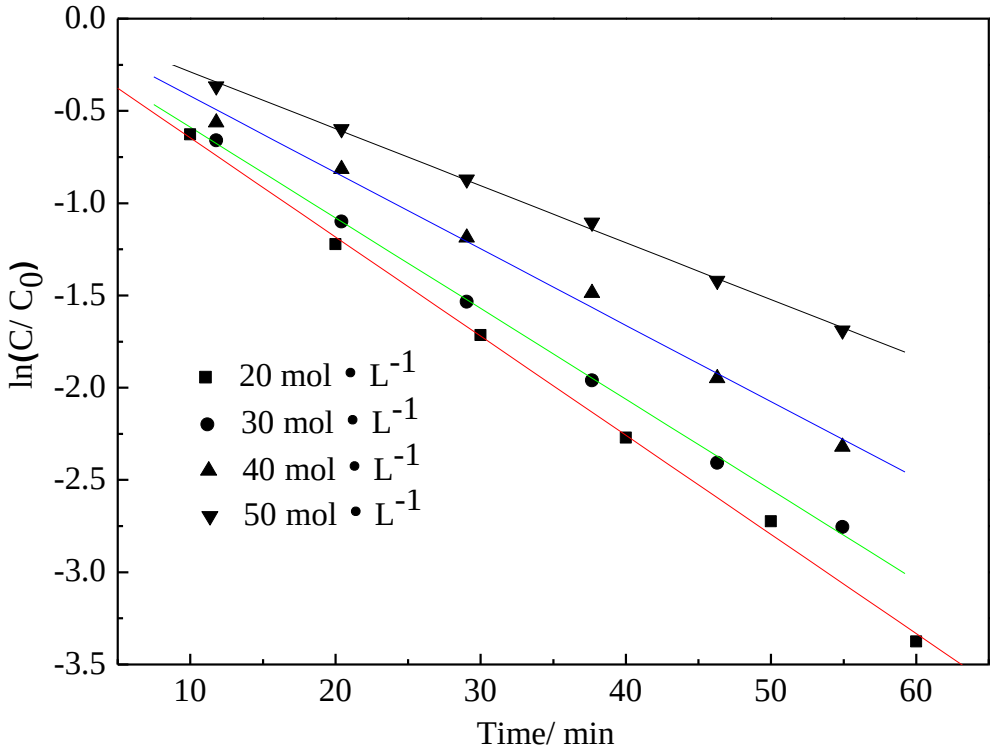

Figure 12. The kinetic fitting curve of MO removal efficiency (Na_2SO_4 0.08 mol·L^{-1}; current density: 40 mA·cm^{-2}; temperature: 25°C; initial pH: 6).

Table 1. The first order reactions kinetic parameters of different concentrations of MO degradation process.

C_0/ mg·L^{-1}	$k''\times10^{-4}$(s^{-1})	R
20	8.955	0.999
30	8.142	0.999
40	6.858	0.997
50	5.113	0.999

The degradation reaction of MO was mainly due to the function of $OH^{\bullet}$, whose removal rate equation can be expressed as [33]:

$$-\frac{dC}{dt} = kC^n[OH^{\bullet}]^m \quad (3)$$

where C is the MO concentration after electrolysing for t min (mg·L^{-1}); [$OH^{\bullet}$] is the OH radical concentration (mg·L^{-1}); m and n are the reaction orders; and k is the reaction kinetic parameters.

The $OH^{\bullet}$ are generated from the water molecules adsorbed on the anode surface. An increase in MO initial concentration would lead to a decrease in $OH^{\bullet}$ yield and then affect the degradation reaction rate. Thus, $k\left[OH^{\bullet}\right]^m$ can be rewritten as $k'C_0^q$:

$$k\left[OH^{\bullet}\right]^m = k'C_0^q = k'' \quad (4)$$

MO removal rate equation can be simplified to equation (5):

$$-\frac{dC}{dt} = k''C^n \quad (5)$$

Based on formula (4), equation (6) can be obtained:

$$\ln k'' = \ln k' + q\ln C_0 \quad (6)$$

Fig. 12 shows that ln(C/C_0) increases with time in a linear relationship, confirming that the electrochemical degradation follows a pseudo first-order reaction, n = 1.

Based on formula (5), equation (8) can be obtained:

$$-\frac{dC}{C} = k''dt \quad (7)$$

$$-\frac{\ln(C-C_0)}{\ln t} = k'' \quad (8)$$

q and k' were obtained by fitting k'' and C_0 in Table 1.

The correlation coefficient 0.99 implies that equation (6) is tenable, and the $OH^{\bullet}$ concentration associated with MO concentration is feasible.

$q = -0.597$, $k' = 6.203\times10^{-3}$ (mg·L^{-1})·s^{-1} can be obtained from the function of the straight line. MO removal rate equation can be expressed as:

$$-\frac{dC}{dt} = 6.203\times10^{-3}C_0^{-0.597}C \quad (9)$$

4. CONCLUSIONS

(1) Nb/PbO_2 electrode surface is dense, uniform and displays a mushroom cloud shape, which mainly composed of β-PbO_2 with a small amount of α-PbO_2. This structure is considered advantages for electrocatalytic applications. Voltammetry showed Nb/PbO_2 electrode has good catalytic effect on degradation of MO.

(2) MO removal efficiency was dependent of the Na_2SO_4 concentration, reaction temperature, pH, and applied current density. Results revealed that the colour and COD removal were respectively achieved 99.6% and 72.6% at the optimal parameters of pH 6.0, 50 $mA \cdot cm^{-2}$ current density, 0.08 $mol \cdot L^{-1}$ Na_2SO_4 concentration, and 30 min electrolysis duration.

(3) The MO electrochemical degradation was mainly caused by OH radical, which followed pseudo first-order reaction process.

ACKNOWLEDGEMENTS
Thank for the jointly funding by the National Natural Science Foundation of China and Shenhua Group Corp (Grant nos. U1261103) and the National Natural Science Foundation of China (Grant nos. 20771080)

References

1. R. H. Liu, G. P. Sheng, M. Sun, G. L. Zang, W. W. Li, Z. H. Tong, F. Dong, M. H. Lam and H. Q. Yu, *Appl. Microbiol. Biotechnol.*, 89 (2011) 201.
2. Z. P. He, Y. C. Shi, L. B. Sun, B. Li and H. J. Nie, *Adv. Mater. Res.*, 669 (2013) 24.
3. S. Figueroa, L.Vázquez and A. Alvarez-Gallegos, *Water Res.*, 43 (2009) 283.
4. V. Prigione, V. Tigini, C. Pezzella, A. Anastasi, G. Sannia and G. C. Varese, *Water Res.*, 42 (2008) 2911.
5. M. H. Zhou, L. C. Lei, Q. Z. Dai, *Chem. Commun.*, 25 (2007) 2645.
6. M. H. Zhou and J. J. He, *Electrochim. Acta.*, 53 (2007) 1902.
7. S. Meric, D. Kaptan and T. Olmez. *Chemosphere*, 54 (2004) 435.
8. D. Valero, J. M. Ortiz, E. Exposito, V. Montiel and A. Aldaz., *Environ. Sci. Technol.*, 44 (2010) 5182.
9. Y. W. Yao, C. M. Zhao, M. Zhao and X. Wang, *J. Hazard. Mater.*, 263 (2013) 726.
10. N. Daneshvar, H. A. Sorkhabi and M. Kobya, *J. Hazard. Mater.*, 112 (2004) 55.
11. L. Ciríaco, C. Anjo, J. Correia, M. J. Pacheco and A. Lopes, *Electrochim. Acta.*, 54 (2009) 1464.
12. C. A. Martínez-Huitle and E. Brillas, *Appl. Catal., B: Environmental*, 87 (2009) 105.
13. M. A. Sanroman, M. Pazos, M. T. Ricart and C. Cameselle, *Chemosphere*, 57 (2004) 233.
14. M. C. Rivera, M. M. D. Jimenez and M. P. E. Gonzalez, *Chemosphere*, 55 (2004) 1.
15. X. Chen, G. Chen and P. L. Yue, *Chem. Eng. Sci.*, 58 (2003) 995.
16. A. Fernandes, A. Morao, M. Magrinho, A. Lopes and I. Goncalves, *Dyes Pigments*, 61 (2004) 287.
17. X. F. Luo, C. H. Yang, Y. Y. Peng, N. W. Pu, M. G. Ger, C. T. Hsieh and J. K. Chang, *J. Mater. Chem. A.*, 3 (2015) 10320.
18. M. Pasta, L. B. Hu, F. La Mantia, Y. Cui, *Electrochem. Commun.*, 19 (2012) 81.
19. L. Szpyrkowicz, C. Juzzolinol, S. N. Kaul, S. Daniele and M. D. De Faveri, *Ind. Eng. Chem. Res.*, 39 (2000) 3241.
20. Y. Samet, S. C. Elaoud, S. Ammar and R. Abdelhedi, *J. Hazard. Mater.*, 138 (2006) 614.
21. Y. Samet, L. Agengui L and R. J. Abdelhédi, *Electroanal. Chem.*, 650 (2010) 152.

22. M. A. Rodrigo, P. A. Michaud, I. Duo, M. Panizza, G. Cerisola and Ch. Comninellis, *J. Electrochem. Soc.*, 148 (2001) D60.
23. M. Panizza and G. Cerisola, *Electrochim. Acta*.,51 (2005) 191.
24. P. A. Michaud, E. Mahe, W. Haenni, A. Perret and Ch. Comninellis, *Electrochem. Solid-State Lett.*, 3 (2000) 77.
25. Y. Wang, Z. Y. Shen and X. C. Chen, *J. Hazard. Mater.*, 178 (2010) 867.
26. C. Q. Zhong, K. J. Wei, W. Q. Han, L. J. Wang, X. Y. Sun and J. S. Li, *J. Electroanal. Chem.*, 2013, 705: 68
27. H. Z. Ma, B. Wang, X. Y. Luo, *J. Hazard. Mater.*, 149 (2007) 492.
28. H. Y. Li, Y. Chen, Y. H. Zhang, W. Q. Han, X. Y. Sun, J. S. Li, L. J. Wang, *J. Electroanal. Chem.*, 689 (2013) 193.
29. Q. Z. Dai, H. Shen, Y. J. Xia, F. Chen, J. D. Wang and J. M. Chen, *Sep. Purif. Technol.*, 104 (2013) 9.
30. S. H. Li, Y. Zhao, J. Chu, W. W. Li, H. Q. Yu and G. Liu, *Electrochim. Acta*, 92 (2013) 93.
31. L. Gomathi Devi, S. Girish Kumar, K. Mohan Reddy and C. Munikrishnappa, *J. Hazard. Mater*, 164 (2009) 459.
32. J. Guo, D. J. Jiang, Y. Wu, P. Zhou, Y. Q. Lan, *J. Hazard. Mater*, 194 (2011) 290.
33. J. Zhao, C. Z. Zhu, J. Lu, C. J. Hu, S. C. Peng, T. H. Chen, *Electrochim. Acta.*, 118 (2014) 169.